

# Zero delay anti-bunching as an entanglement signature for plasmonically coupled driven qubits

Eugene Dumitrescu<sup>1,2,3</sup> and Benjamin Lawrie<sup>1,2</sup>

<sup>1</sup> *Quantum Computing Institute, Oak Ridge National Laboratory, Oak Ridge, TN 37831*

<sup>2</sup> *Quantum Information Science Group, Oak Ridge National Laboratory, Oak Ridge, TN 37831*

<sup>3</sup> *Bredesen Center for Interdisciplinary Research, University of Tennessee, Knoxville, TN 37996*

Dissipative entanglement generation protocols embrace environmental interactions in order to generate long-lived entangled states. In this letter, we report on anti-bunching in the second order correlation function for a pair of actively driven quantum emitters coupled to a shared dissipative plasmonic reservoir. We find that anti-bunching is a universal signature for entangled states generated by dissipative means and examine its use as an entanglement diagnostic. We discuss the experimental validation of anti-bunching on realistic timescales, determined by an effective two-qubit Rabi frequency, and analyze the robustness of entanglement generation with respect to perturbations in local detunings, couplings, and driving fields.

*Introduction.*— Quantum decoherence results from interactions with unknown or uncontrollable environmental degrees of freedom. This process, by which quantum information deteriorates due to environmental interactions, has been coined information leakage[1]. It follows that quantum information processing systems should be completely isolated from leaky environments. However, such a task has proven to be quite difficult, and as a consequence, a variety of techniques have been developed to combat the effects of decoherence[2]. With the fault tolerant threshold theorem [3] providing a route to overcome decoherence, quantum error correction protocols [2, 4–9], dynamical decoupling protocols [10], and decoherence suppressing quantum control techniques [11, 12] have all seen substantial progress.

Dissipative driven entanglement (DDE) techniques provide a different and complimentary route to quantum state engineering [13]. In this paradigm, entanglement is stabilized[14] and computations are performed[15] by leveraging select dissipative pathways which are naively assumed to impede long term quantum coherence. Early experimental DDE progress has been achieved in trapped ion [16], atomic ensemble [17, 18], and superconducting [19] qubit platforms.

Concurrently, a new quantum information processing platform based on the quantum theory of plasmons has rapidly matured in recent years [20, 21]. The first demonstration of plasmonically mediated entanglement [22] stimulated developments in both discrete [20] and

continuous [23, 24] plasmonic quantum variables. More recently, squeezed states of light have enabled ultra-trace plasmonic sensing [25, 26], while plasmonic mode volumes orders of magnitude below the diffraction limit have enabled Purcell factors exceeding  $10^3$  in the weak coupling limit[27] and vacuum Rabi splitting in the strong coupling limit [28]. These plasmonic analogs to photonic cavity QED provide a framework for the development of nanoscale architectures with ultrafast coupling dynamics capable of operation at ambient temperatures.

Despite substantial theoretical progress [29–41], dissipative entanglement generation has yet to be observed in plasmonic platforms, partially due to the technical difficulty of integrating plasmonic components with standard readout and control technologies. It is therefore tremendously important to develop simple alternative entanglement metrics for nascent plasmon based DDE experiments. In this letter we propose the use of the  $g^{(2)}(\tau)$  second order correlation function as such a metric. Namely, we demonstrate that the degree of anti-bunching, of the photons radiated from our setup, is strongly correlated with the degree of entanglement that is dissipatively generated. We show how manipulating the local qubit driving amplitudes may be used to reduce the two qubit Rabi frequency, thus extending the anti-bunching width to timescales which are currently experimentally accessible.

*Theory.*— We consider a physical setup, illustrated in Fig. 1, consisting of a pair of qubits placed in close proximity to the near-field of a surface plasmon mode supported on a metallic nanowire. Qubit-qubit interactions are thus mediated by a plasmonic boson reservoir. The bare plasmon Hamiltonian is  $H_{pls} = \int d\mathbf{r} \int_0^\infty d\omega \hbar \omega \hat{a}^\dagger(\mathbf{r}, \omega) \hat{a}(\mathbf{r}, \omega)$ , where  $\hat{a}(\mathbf{r}, \omega)$  and  $\hat{a}^\dagger(\mathbf{r}, \omega)$  are the destruction and creation operators for elementary plasmonic excitations which satisfy bosonic commutation relations. A resonant or near-resonant mode may be treated as an oscillator  $H_{pls} = \hbar \omega_a \hat{a}^\dagger \hat{a}$  with a principal frequency  $\omega_a$ . The qubit Hamiltonian

<sup>1</sup> This manuscript has been authored by UT-Battelle, LLC, under Contract No. DE-AC0500OR22725 with the U.S. Department of Energy. The United States Government retains and the publisher, by accepting the article for publication, acknowledges that the United States Government retains a non-exclusive, paid-up, irrevocable, world-wide license to publish or reproduce the published form of this manuscript, or allow others to do so, for the United States Government purposes. The Department of Energy will provide public access to these results of federally sponsored research in accordance with the DOE Public Access Plan.

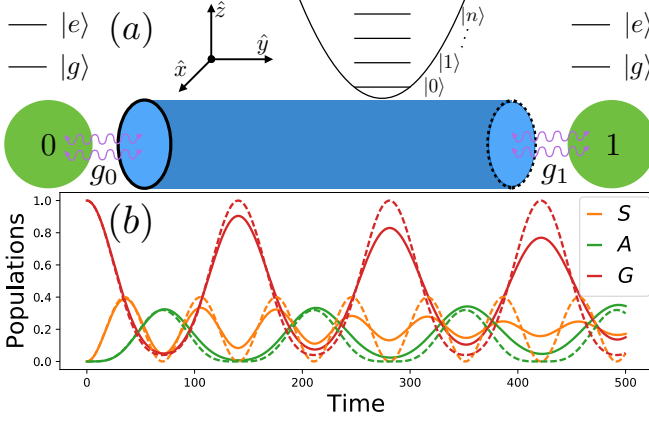


FIG. 1. (a) Schematic diagram of the setup described by Eq. 1. (b) Dashed (solid) lines show the numerical (effective analytic) populations of the ground (G), symmetric (S), and antisymmetric (A) states for a system with physical parameters (and their effective counterparts without dissipation):  $\Delta_0 = -\Delta_1 = 0.02$ ,  $g_0 = g_1 = 0.02$ ,  $\eta_0 = \eta_1 = 0.02$ ,  $\gamma_d = 2\gamma_r = 1e^{-8}$ , and  $\gamma_a = 50THz$ . All parameters are reported as ratios of  $\gamma_a$ .

reads  $H_i = \hbar\omega_i\hat{\sigma}_i^+\hat{\sigma}_i^-$ , where  $i = 0, 1$  indexes the emitters which are modeled as two level systems with  $\hat{\sigma}_i^\pm$  being the Pauli ladder operators,  $\hat{\sigma}^\pm = \hat{\sigma}^x \pm i\hat{\sigma}^y = |e\rangle\langle g|(|g\rangle\langle e|)$ . The qubits could be implemented by a variety of solid state platforms, for example, as semiconductor quantum dots[42, 43]. We do not restrict ourselves to a specific qubit platform, but note that our results are generally applicable given appropriate plasmonic mode matching, which may be tuned by adjusting the nanowire geometry [44–46]. Defining the plasmonic and TLS dipole operators as  $\hat{d}_a = \hat{a}^\dagger + \hat{a}$  and  $\hat{d}_i = \hat{\sigma}_i^+ + \hat{\sigma}_i^-$ , the emitter-reservoir coupling is modeled by the interaction  $H_{int} = \sum_i g_i \hat{d}_a \cdot \hat{d}_i$ , where  $g_i \equiv (\mu_i \cdot E_i)/\hbar$  is the dipole interaction strength in which we have absorbed all physical constants, i.e. the emitter transition dipole moment  $\mu_i$  and local plasmon electric field magnitude  $E_i = \sqrt{\frac{\hbar\omega_a}{2\epsilon_0 V}}$  where  $V$  is the plasmon mode volume. Plasmonic elements behave as lossy electromagnetic cavities in the both the weak and strong QED regimes [21, 27–29, 46]. Finally,  $H_D = -\sum_i (\eta_i e^{i\Omega_i t} \hat{\sigma}_i^+ + H.c.) - (\eta_a e^{i\Omega_a t} \hat{a}^\dagger + H.c.)$  models transitions being driven by external fields with amplitudes  $\eta_i(a)$  and frequencies  $\Omega_i(a)$ . Transforming to the co-rotating reference frame, with detunings  $\Delta_{i(a)} = \hbar(\omega_{i(a)} - \Omega_{i(a)})$ , and applying the rotating wave approximation, the total Hamiltonian becomes,

$$H_{tot} = \sum_{i=0,1} \left[ \Delta_i \hat{\sigma}_i^+ \hat{\sigma}_i^- - \eta_i \hat{d}_i - g_i (\hat{\sigma}_i^+ \hat{a} + \hat{\sigma}_i^- \hat{a}^\dagger) \right] \quad (1)$$

$$+ \Delta_a \hat{a}^\dagger \hat{a} - \eta_a \hat{d}_a.$$

t The effects of dissipation are modeled by treating the dynamics within the Lindblad master equation formal-

ism,

$$\dot{\rho} = -i[H_{tot}, \rho] + \sum_k \gamma_k (L_k \rho L_k^\dagger - \frac{1}{2} \{L_k^\dagger L_k, \rho\}) \quad (2)$$

where we have taken  $\hbar = 1$  and  $L_k$  represent the various subsystem dissipation operators. Explicitly, we consider the following Lindblad terms: (i) plasmonic relaxation  $L_a \equiv \hat{a}$  occurring at a typical frequency  $\gamma_a \leq 50THz$ [47], (ii) emitter relaxation  $L_{r,i} \equiv \hat{\sigma}_i^+$  at a rate  $\gamma_r = 2.5MHz$ , and (iii) emitter dephasing  $L_{d,i} \equiv \hat{\sigma}_i^z$  at double the relaxation rate  $\gamma_d = 5MHz$ .

*Effective Dynamics.*— In the weak coupling regime,  $g_0, g_1, \eta_0, \eta_1 \ll \gamma_a$ , plasmon populations quickly saturate as relaxations dominate qubit mediated excitations. The the reservoir modes may therefore be adiabatically eliminated as follows[41]. The Heisenberg equations of motion for the field degrees of freedom under the dynamics of Eqs. 1 and 2 are

$$\begin{aligned} \dot{\sigma}_i^z &= i[2g_i(\sigma_i^+ a - \sigma_i^- a^\dagger) + 2\eta_i(\sigma_i^+ - \sigma_i^-)] \quad (3) \\ &\quad - \gamma_i(\mathbb{I} - \sigma_z) \\ \dot{\sigma}_i^- &= -i[\Delta_i \sigma_i^- + (g_i a + \eta_i) \sigma_i^z] - \gamma_i \sigma_i^- / 2 \\ \dot{a} &= i[\eta_a - \Delta_a a + g_0 \sigma_0^- + g_1 \sigma_1^-] - \gamma_a a / 2. \end{aligned}$$

Setting  $\dot{a} = 0$  and substituting the resulting expression into the the first two lines of Eq. 3 we find adiabatic Heisenberg equations of motion, which can in turn be viewed as arising from an effective two qubit Hamiltonian with non-local dissipation terms. The effective Hamiltonian,  $H_{qb} = \sum_i [\tilde{\Delta}_i \hat{\sigma}_i^+ \hat{\sigma}_i^- - \tilde{\eta}_i \hat{d}_i] - \tilde{g}(\hat{\sigma}_0^+ \hat{\sigma}_1^- + \hat{\sigma}_1^+ \hat{\sigma}_0^-)$ , is defined in terms of the following effective parameters:  $\tilde{\Delta}_i = \Delta_i - g_i^2 \Delta_a / Z$ ,  $\tilde{\eta}_i = \eta_i + g_i \Delta_a \eta_a / Z$ , and  $\tilde{g} = g_0 g_1 \Delta_a / Z$ , where  $Z = (\gamma_a / 2)^2 + \Delta_a^2$ . The effective dissipations are described by  $\sum_{ij=0,1} \tilde{\gamma}_{ij} / 2 [2\sigma_i^- \rho \sigma_j^+ - \{\sigma_j^+ \sigma_i^-, \rho\}]$ , with single qubit relaxations occurring at a renormalized rate  $\tilde{\gamma}_{ii} = \gamma_i + g_i^2 \gamma_a / Z$  and collective reservoir mediated relaxations occurring at the rate  $\tilde{\gamma}_{ij} = g_0 g_1 \gamma_a / Z$ . Transforming to the Dicke basis,  $|E\rangle = |ee\rangle$ ,  $|S\rangle = |eg\rangle + |ge\rangle$ ,  $|A\rangle = |eg\rangle - |ge\rangle$ ,  $|G\rangle = |gg\rangle$ , and defining the effective (anti)symmetric drivings  $\eta_\pm = (\tilde{\eta}_0 \pm \tilde{\eta}_1) / \sqrt{2}$  and energies  $\Delta_\pm = (\tilde{\Delta}_0 \pm \tilde{\Delta}_1) / 2$ , the Hamiltonian reads

$$H_D = \Delta_E |E\rangle\langle E| + \Delta_S |S\rangle\langle S| + \Delta_A |A\rangle\langle A| \quad (4)$$

$$+ \Delta_- (|A\rangle\langle S| + |S\rangle\langle A|)$$

$$- \eta_- (|S\rangle\langle G| + |S\rangle\langle E| + H.c.)$$

$$- \eta_+ (|A\rangle\langle G| - |A\rangle\langle E| + H.c.).$$

where  $\Delta_E = 2\Delta_+$ ,  $\Delta_S = \Delta_+ + \tilde{g}$ , and  $\Delta_A = \Delta_+ - \tilde{g}$ . Taking anti-symmetric detunings and equal drivings the effective parameters reduce to  $\tilde{\Delta}_i = \Delta_i$ ,  $\tilde{\eta}_i = \eta_i$ ,  $\tilde{g} = 0$ ,  $\tilde{\gamma}_{ii} = \gamma_i + 4g_i^2 / \gamma_a$ , and  $\tilde{\gamma}_{ij} = 4g_0 g_1 / \gamma_a$ . The resulting pure state populations, e.g. with  $\rho(0) = |G\rangle\langle G|$ , oscillate with an effective two qubit Rabi frequency  $\Omega = \sqrt{(\Delta/2)^2 + \eta^2}$

as  $\rho_E(t) = (\Delta^2 + \eta^2 \cos(2t\Omega) - \Omega^2)/4\Omega^4$ ,  $\rho_S(t) = \eta^2 \sin^2(2t\Omega)/2\Omega^2$ ,  $\rho_A(t) = 2\Delta^2\eta^2 \sin^4(t\Omega)/\Omega^4$ ,  $\rho_G(t) = (\Delta^2 + \eta^2 \cos(2t\Omega) + \Omega^2)/4\Omega^4$ , and are illustrated by the solid lines in Fig. 1.

The dashed populations in Fig. 1 are calculated by numerically solving Eq. 2 for the full system and can be understood as follows. As discussed above, the excited state  $|E\rangle$  relaxes to the singly excited state  $|eg(ge)\rangle$  at a rate  $\tilde{\gamma}_{00(11)}$ . However, in the Dicke basis, relaxation from the bi-excited state to the symmetric (antisymmetric) state occurs at the rate  $\gamma_{S(A)} = \sum_i \tilde{\gamma}_{ii}/2 \pm \gamma_{ij}$ . Ignoring Hamiltonian dynamics for the moment, the populations are coupled as  $\dot{\rho}_{SS} = (\rho_{EE} - \rho_{SS})\gamma_S$  and  $\dot{\rho}_{AA} = (\rho_{EE} - \rho_{AA})\gamma_A$ . Thus, the dashed lines in Fig. 1 and the eventual steady states, can be driven by symmetric pumping described by Eq. 4 augmented by super- and sub-radiant dissipation from the states  $|S\rangle$ , and  $|A\rangle$  respectively. As discussed below, the entangled state  $|A\rangle$  is a fixed point solution to these dynamics.

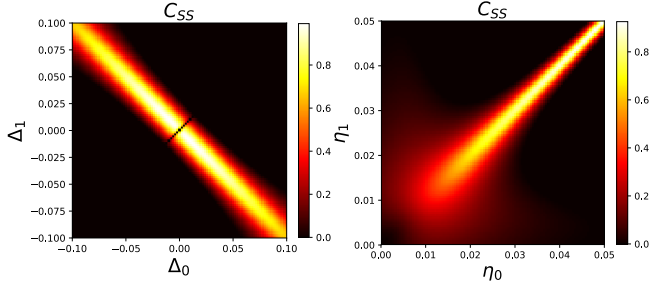


FIG. 2. Concurrence as a function of (a) qubit detunings  $\Delta_{0,1}$  with equal qubit drivings  $\eta_0 = \eta_1 = 0.05$  and (b) qubit driving amplitudes  $\eta_{0,1}$  with asymmetric qubit detunings  $\Delta_0 = -\Delta_1 = 0.01$ . Symmetric drivings and couplings with anti-symmetric detunings yields near unity concurrence steady states  $\rho_{ss} \approx |A\rangle\langle A|$ . Parameters common to both panels are coupling strengths  $g_0 = g_1 = 0.05$  and plasmon detuning and driving  $\Delta_a = \eta_a = 0$ .

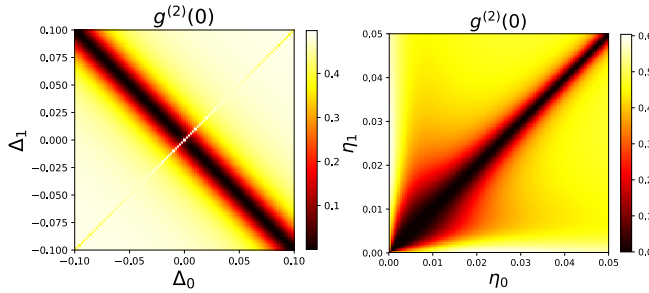


FIG. 3. Zero delay anti-bunching  $g^{(2)}(0)$  as a function of (a) qubit detunings  $\Delta_{0,1}$  and (b) qubit drive amplitudes  $\eta_{0,1}$  using parameters reported in Fig. 2. Dark bands illustrate the zero delay anti-bunching signal, which overlaps strongly with high concurrence regions.

We now explore steady state characteristics as a func-

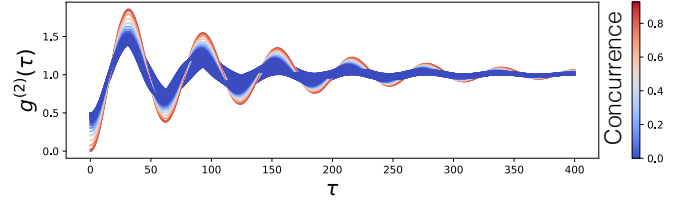


FIG. 4. Steady state  $g^{(2)}(\tau)$  correlation function as the driving amplitude  $\eta_0$  sweeps through the range  $[0.04, 0.06]$ . Over this range the concurrence evolves (see colorbar) from 0 to 1, where a zero-delay anti-bunching is seen, and back to 0, with a nonzero  $g^{(2)}(0)$ . Other Hamiltonian parameters, as ratios of  $\gamma_a$ , are  $\Delta_0 = -\Delta_1 = 0.02$ ,  $g_0 = g_1 = 0.05$ , and  $\eta_1 = 0.05$ .

tion of the parameter space defined in Eq. 1. Fixed point entanglement is characterized by Woote's concurrence  $C$  [48]. The concurrence of a two qubit state  $\rho$  is  $C(\rho) = \max\{0, \lambda_1 - \lambda_2 - \lambda_3 - \lambda_4\}$  where  $\lambda_j$  are the sorted eigenvalues of  $\rho\tilde{\rho}$ , with the spin-flipped conjugate state  $\tilde{\rho} = \sigma_1^y \sigma_2^y \rho^* \sigma_2^y \sigma_1^y$ .  $C$  ranges between 0, for product states, and 1, for maximally entangled states. As indicated by our earlier discussion and illustrated in Fig. 2, unit concurrence is readily achievable for systems with approximately equal couplings and driving fields as well as approximately anti-symmetric qubit detuning. In all cases, the pair of qubits evolves to the anti-symmetric entangled state  $|A\rangle$  [39, 41].

*$g^{(2)}(\tau)$  as an entanglement witness*— We now investigate the use of the second order temporal correlation function to verify entanglement generation in our system. Entanglement is typically validated by an ensemble of computational basis state measurements that are classically post-processed to either perform state tomography[49, 50] or demonstrate a quantum inequality violation[51, 52]. Tomographic state readout has been successfully performed for dissipatively entangled trapped ions [16] using specialized readout mechanisms. However, for nascent plasmonic technologies, it is worthwhile to develop simple experimental signatures consistent with entangled states, without the complicated readout electronics needed to perform full state tomography. In this context, the temporal correlations of emitted light has been suggested as an alternative entanglement signature [39, 53, 54]. Below we confirm that the second order correlation function successfully discriminates between entangled, arising in the form  $|A\rangle$ , and unentangled steady states generated by our protocol.

The second order correlation function measures the degree to which a system is temporally correlated. For stationary processes invariant under time translation, as is the case for steady states, the correlation function is defined as

$$g^{(2)}(\tau) = \frac{\langle a^\dagger(t)a^\dagger(t+\tau)a(t+\tau)a(t) \rangle}{\langle a^\dagger(t)a(t) \rangle^2}. \quad (5)$$

In the context of quantum optics,  $g^{(2)}(\tau)$  has the simple and intuitive interpretation of the normalized probability that two photons, whose emission times differ by  $\tau$ , are detected at a point in space. A Hanbury Brown Twiss (HBT) interferometer [55] can be used to measure this quantity. In a modern HBT interferometer a 50/50 beamsplitter is used to send a light source to a pair of single photon counting detectors, and high speed electronics tag the arrival times of photons at each detector, with temporal resolution as fast as 1 picosecond.

In order to calculate  $g^{(2)}(\tau)$  let us now combine continuous time evolution with a discrete quantum jump model. Consider a steady state  $\rho_{ss}$  of Eq. 2, whose concurrence is plotted in Fig. 2, which spontaneously emits a single photon from either qubit. An emission event originating from the  $i^{\text{th}}$  qubit corresponds mathematically to the application of a destruction operator  $\sigma_i^-$  which projectively maps the post-emission state to  $\rho_i(0) = \hat{\sigma}_i^{(-)} \rho_{ss} \hat{\sigma}_i^{(+)} / \text{Tr} [\hat{\sigma}_i^{(-)} \rho_{ss} \hat{\sigma}_i^{(+)}]$ . Defining  $\rho_i(\tau)$  as  $\rho_i(0)$  evolved from  $t = 0$  to  $t = \tau$  according to Eq. 2, the probability for a second emission from the  $j^{\text{th}}$  qubit at time  $\tau$  is then  $\text{Tr} [\hat{n}_j \rho_i(\tau)]$ , where  $\hat{n}_j = \hat{\sigma}_j^{(+)} \hat{\sigma}_j^{(-)}$  is the qubit number operator. Summing over all possible emission configurations gives us

$$g^{(2)}(\tau) = \sum_{ij} \text{Tr} [\hat{n}_j \rho_i(\tau)]. \quad (6)$$

In Fig. 4 we present  $g^{(2)}(\tau)$  as a function of steady state concurrence by sweeping the driving amplitude  $\eta_0$  across the range  $[0.04, 0.06]$ , such that the concurrence sweeps from 0 to 1 and back to 0 (see Fig. 2). We observe a zero delay anti-bunching dip emerge and disappear as the driving intensity modulation increase and decrease the concurrence. Generally, this correlated anti-bunching signature appears for all dissipatively generated entangled steady states as seen in Fig. 3, where we plot the  $g^{(2)}(0)$  signal versus the single qubit parameters.

An anti-bunching dip is not a general entanglement metric for arbitrary quantum states, but it is a universal feature shared by sub-radiance generated entangled steady states. The anti-bunching robustness is rooted in the fact that a single quantum is shared between two qubits comprising  $|A\rangle$ . In contrast, product states sharing a single quantum, e.g.  $|eg\rangle$  or  $|ge\rangle$ , are unstable under the dynamics considered with only linear combinations being steady state solutions. Further,  $g^{(2)}(\tau)$  is unaffected by states including statistical mixtures of  $|G\rangle$ , while bi-excited states  $|E\rangle$  source, with high probability, two small delay emissions that reduce anti-bunching. Anti-bunching is therefore maximal for steady state with large support on  $|A\rangle$ , the only stable single excitation subspace.

While anti-bunching is an attractive entanglement signature due to its simplicity, its observation is non-trivial due to the fast time-scales inherited from the plasmonic

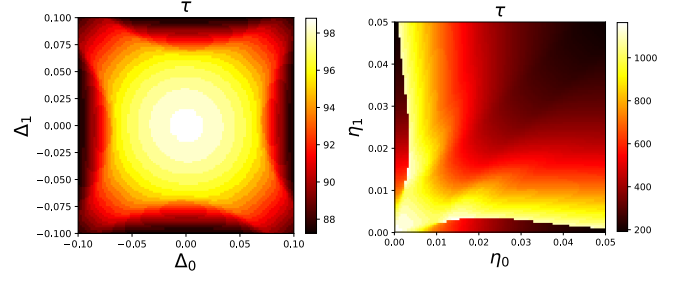


FIG. 5. Oscillation timescales for anti-bunching signal as a function of (a) qubit detunings  $\Delta_{0,1}$  and (b) qubit drive amplitudes  $\eta_{0,1}$ . Timescales reported are in units of  $T = 1/\gamma_a$  with remaining parameters as in Fig. 2. Entangled region around  $\eta_0 = \eta_1 = 0.03$  displays a characteristic bunching timescale  $T_{AB} \sim 10ps$ .

reservoir. After each radiative decay event, the two qubit system flows back to its steady state solution as described earlier. Hence the width of the  $g^{(2)}(0)$  anti-bunching dip is inversely proportional to the population oscillation Rabi frequency  $\Omega$ . Tunable driving frequencies are therefore critical to observing anti-bunching on experimentally accessible timescales. While nonlinear mixing with femtosecond laser sources could in principle enable the detection of sub-picosecond dynamics in  $g^{(2)}(\tau)$ , conventional HBT interferometry is limited by the 1 ps temporal resolution of state-of-the-art time tagging electronics. To that end, we numerically calculate the oscillation timescales by Fourier transforming the  $g^{(2)}(\tau)$  signal into the frequency domain and identifying the characteristic driving frequency, which fixes the anti-bunching timescale. The timescales are provided in the Fig. 5 color-maps, as a function of detuning and driving amplitudes, with normalized time in units of  $T = 1/(\pi * \gamma_a) \approx 6fs$  reported in the color legend. Anti-bunching timescales in the  $\sim 10ps$  range for entangled states are easily experimentally realizable, e.g. for small driving fields around  $\eta_0 = \eta_1 \approx 0.03$ .

*Conclusion and discussion*— In this letter we have examined the entanglement characteristics of steady states generated by a pair of qubits subject to a dissipative plasmonic reservoir. We have found that maximally entangled steady states are routinely achievable by appropriately tuning qubit detunings, couplings and driving frequencies. Further, the entanglement was found to be robust against small perturbations in the tuning parameters, which need only be approximately symmetric (couplings, drivings) or anti-symmetric (detunings) in order to generate high concurrence states. We have also examined entanglement detection by an anti-bunching signature in the second order correlation function which is routinely measured by means of a Hanbury Brown Twiss interferometer. By correlating this effect with the steady state concurrence, we discussed how the zero-delay anti-bunching serves as a robust entanglement sig-

nature. Importantly, we have also demonstrated that dynamics driven by weak fields allows the anti-bunching signature to persist on  $\mathcal{O}(ps)$  timescales which pave the way to experimental detection using currently available experimental techniques. This robustness against microscopic perturbations and unentangled fixed point states cements the  $g^{(2)}(\tau)$  correlation function as a simple and practical measure of steady state entanglement generation.

*Acknowledgements.*— The authors thank F. Mohiyaddin for discussions and careful reading of the manuscript. E. D. acknowledges support from the Intelligence Community Postdoctoral Research Program. Research sponsored by the Intelligence Community Postdoctoral Research Fellowship and the Laboratory Directed Research and Development Program of Oak Ridge National Laboratory, managed by UT-Battelle, LLC, for the U.S. Department of Energy. This manuscript has been authored by UT-Battelle, LLC, under Contract No. DE-AC0500OR22725 with the U.S. Department of Energy.

- 
- [1] M. A. Nielsen and I. L. Chung, *Quantum Computation and Quantum Information*, Cambridge University Press (2010)
  - [2] B. M. Terhal, “Quantum error correction for quantum memories”, *Rev. Mod. Phys.* **87**, 307 (2015)
  - [3] “Fault-tolerant quantum computation with constant error”, D. Aharonov and M. Ben-Or, *Proc. 29th Ann. ACM Symp. on Theory of Computation*, ACM, New York, (1998)
  - [4] P. W. Shor, *Phys. Rev. A* **52**, R 2493(R) (1995)
  - [5] A. R. Calderbank, E. M. Rains, P. W. Shor, and N. J. A. Sloane, “Quantum Error Correction via Codes over  $GF(4)$ ” *IEEE Trans. Inform. Theory*, **44** 1369-1387 (1998).
  - [6] R. Laflamme, C. Miquel, J. P. Paz, and W. Zurek, “Perfect Quantum Error Correcting Code” *Phys. Rev. Lett.* **77**, 198 (1996)
  - [7] A. M. Steane, “Error correcting codes in quantum theory” *Phys. Rev. Lett.* **77**, 793-797 (1996)
  - [8] D. Gottesman, Caltech Thesis, arXiv:quant-ph/9705052, (1997)
  - [9] A. Y. Kitaev, “Fault-tolerant quantum computation by anyons” *Annals of Physics* **303** 2-30 (2003)
  - [10] “Dynamical Decoupling of Open Quantum Systems”, L. Viola, E. Knill, S. Lloyd, *Phys. Rev. Lett.* **82**, 2417 (1999)
  - [11] “Quantum feedback control and classical control theory”, A. C. Doherty, S. Habib, K. Jacobs, H. Mabuchi, and S. M. Tan, *Phys. Rev. A* **62**, 012105 (2000)
  - [12] “Quantum control theory and applications: A survey”, D. Dong, I. R. Petersen, *IET Control Theory & Applications*, **4**, 12, (2010)
  - [13] “Quantum computation and quantum-state engineering driven by dissipation,” F. Verstraete, M. M. Wolf, and J. I. Cirac, *Nat. Phys.* **5**, 633 (2009)
  - [14] “Driving two atoms in an optical cavity into an entangled steady state using engineered decay”, F. Reiter, M. J. Kastoryano, A. S. Sorensen, *New Journal of Physics* **14** 053022 (2012)
  - [15] “Precisely Timing Dissipative Quantum Information Processing,” M. J. Kastoryano, M. M. Wolf, and J. Eisert, *Phys. Rev. Lett.* **110**, 110501 (2013)
  - [16] “Dissipative production of a maximally entangled steady state of two quantum bits”, Y. Lin, J. P. Gaebler, F. Reiter, T. R. Tan, R. Bowler, A. S. Sorensen, D. Leibfried, and D. J. Wineland, *Nature* **504**, 415-418 (2013)
  - [17] “Dissipatively driven entanglement of two macroscopic atomic ensembles,” C. A. Muschik, E. S. Polzik, and J. I. Cirac, *Phys. Rev. A* **83**, 052312 (2011)
  - [18] “Entanglement generated by dissipation and steady state entanglement of two macroscopic objects”, H. Krauter, C. A. Muschik, K. Jensen, W. Wasilewski, J. M. Petersen, J. Ignacio Cirac, E. S. Polzik, *Phys. Rev. Lett.* **107**, 080503 (2011)
  - [19] “Comparing and Combining Measurement-Based and Driven-Dissipative Entanglement Stabilization” Y. Liu, S. Shankar, N. Ofek, M. Hatridge, A. Narla, K. M. Sliwa, L. Frunzio, R. J. Schoelkopf, and M. H. Devoret *Phys. Rev. X* **6** 011022 (2016)
  - [20] “Quantum Plasmonics” M. S. Tame, K. R. McEnery, S. K. Ozdemir, J. Lee, S. A. Maier, and M. S. Kim, *Nature Physics* **9**, 329-340 (2013)
  - [21] “Cavity quantum electrodynamics in application to plasmonics and metamaterials”, P. Ginzburg, *Reviews in Physics* **1** 120-139 (2016)
  - [22] “Plasmon-assisted transmission of entangled photons”, E. Altewischer, M. P. van Exter and J. P. Woerdman, *Nature* **418**, 304-306 (18 July 2002)
  - [23] “Extraordinary Optical Transmission of Multimode Quantum Correlations via Localized Surface Plasmons”, B. J. Lawrie, P. G. Evans, and R. C. Pooser, *Phys. Rev. Lett.* **110**, 156802, (2013)
  - [24] “Toward quantum plasmonic networks”, M. W. Holtfrerich, M. Dowran, R. Davidson, B. J. Lawrie, R. C. Pooser, and A. M. Marino, *Optica* Vol. 3, Issue 9, pp. 985-988 (2016)
  - [25] “Quantum plasmonic sensing”, W. Fan, B. J. Lawrie, and R. C. Pooser, *Phys. Rev. A* **92**, 053812 (2015)
  - [26] “Plasmonic Trace Sensing below the Photon Shot Noise Limit”, R. C. Pooser and B. Lawrie, *ACS Photonics*, **3** (1), pp 8-13 (2016)
  - [27] “Probing the mechanisms of large Purcell enhancement in plasmonic nanoantennas”, G. M. Akselrod, et. al., *Nature Photonics*, **8**, 835-840, (2014).
  - [28] “Single-molecule strong coupling at room temperature in plasmonic nanocavities”, R. Chikkaraddy, et. al., *Nature* **535**, 7610 (2016).
  - [29] “Weak and strong coupling regimes in plasmonic QED”, T. Hummer, F. J. Garcia-Vidal, L. Martin-Moreno, and D. Zueco, *Phys. Rev. B* **87**, 115419 (2013)
  - [30] “Surface plasmons in a metal nanowire coupled to colloidal quantum dots: Scattering properties and quantum entanglement”, G.-Y. Chen, N. Lambert, C.-H. Chou, Y.-N. Chen, and F. Nori, *Phys. Rev. B* **84**, 045310 (2011)
  - [31] “Multifrequency multi-qubit entanglement based on plasmonic hot spots”, J. Ren, T. Wu, and X. Zhang, *Sci. Rep.* **5**, 13941 (2015)
  - [32] “Nanoshell-mediated robust entanglement between coupled quantum dots”, J. Hakami and M. S. Zubairy, *Phys. Rev. A* **93**, 022320 (2016)

- [33] “Dissipative dynamics of a solid-state qubit coupled to surface plasmons: From non-Markov to Markov regimes”, A. Gonzalez-Tudela, F. J. Rodriguez, L. Quiroga, and C. Tejedor, *Phys. Rev. B* **82**, 115334 (2010)
- [34] “Robust-to-loss entanglement generation using a quantum plasmonic nanoparticle array”, C. Lee, M. Tame, C. Noh, J. Lim, S. A. Maier, J. Lee, and D. G. Angelakis, *New Jour. Phys.*, Vol. **15**, (2013)
- [35] “Transient and steady-state entanglement mediated by three-dimensional plasmonic waveguides”, S. A. H. Gangaraj, A. Nemilentsau, G. W. Hanson, and S. Hughes, *Optics Express* Vol. 23, Issue 17, pp. 22330-22346 (2015)
- [36] “Entanglement of two qubits mediated by a localized surface plasmon”, K. V. Nerkararyan and S. I. Bozhevolnyi, *Phys. Rev. B* **92**, 045410 (2015)
- [37] “Entanglement of two, three, or four plasmonically coupled quantum dots”, M. Otten, R. A. Shah, N. F. Scherer, M. Min, M. Pelton, and S. K. Gray, *Phys. Rev. B* **92**, 125432 (2015)
- [38] “Origins and optimization of entanglement in plasmonically coupled quantum dots”, M. Otten, J. Larson, M. Min, S. M. Wild, M. Pelton, and S. K. Gray, *Phys. Rev. A* **94**, 022312 (2016)
- [39] “Dissipation-driven generation of two-qubit entanglement mediated by plasmonic waveguides”, D. Martin-Cano, A. Gonzalez-Tudela, L. Martin-Moreno, F. J. Garcia-Vidal, C. Tejedor, and E. Moreno, *Phys. Rev. B* **84**, 235306 (2011)
- [40] “Entanglement of Two Qubits Mediated by One-Dimensional Plasmonic Waveguides” A. Gonzalez-Tudela, D. Martin-Cano, E. Moreno, L. Martin-Moreno, C. Tejedor, and F. J. Garcia-Vidal *Phys. Rev. Lett.* **106**, 020501 (2011)
- [41] “Dissipation-driven entanglement between qubits mediated by plasmonic nanoantennas,” J. Hou, K. Slowik, F. Lederer, and C. Rockstuhl, *Phys. Rev. B* **89**, 235413 (2014)
- [42] R. Hanson, L. P. Kouwenhoven, J. R. Petta, S. Tarucha, and L. M. K. Vandersypen, “Spins in few-electron quantum dots”, *Rev. Mod. Phys.* **79**, 1217 (2007).
- [43] P. Lodahl, S. Mahmoodian, and S. Stobbe, “Interfacing single photons and single quantum dots with photonic nanostructures”, *Rev. Mod. Phys.* **87**, 347 (2015).
- [44] “Quantum optics with surface plasmons”, D. E. Chang, A. S. Sørensen, P. R. Hemmer, and M. D. Lukin, *Phys. Rev. Lett.* **97**, 5, (2006).
- [45] “Plasmon slot waveguides: Towards chip-scale propagation with subwavelength-scale localization”, J. A. Dionne, L. A. Sweatlock, H. A. Atwater, and A. Polman, *Phys. Rev. B* **73**, 035407 (2006).
- [46] “Single-molecule optomechanics in “picocavities” ” F. Benz, et. al., *Science*, **354**, 6313, (2016).
- [47] “Ultrafast Plasmonic Control of Second Harmonic Generation”, R. B. Davidson II, A. Yanchenko, J. I. Ziegler, S. M. Avanesyan, B. J. Lawrie, and R. F. Haglund Jr. *ACS Photonics*, **3** (8), pp 1477-1481 (2016)
- [48] “Entanglement of Formation of an Arbitrary State of Two Qubits”, W. K. Wootters, *Phys. Rev. Lett.* **80** 2245 (1998)
- [49] J. F. Poyatos, J. I. Cirac, P. Zoller, “Complete Characterization of a Quantum Process: The Two-Bit Quantum Gate”, *Phys. Rev. Lett.* **78** 390 (1997).
- [50] I. L. Chuang and M. A. Nielsen “Prescription for experimental determination of the dynamics of a quantum black box”, *Journal of Modern Optics*, **44** 11-12, 2455-2467 (1997).
- [51] “On the EPR paradox”, J. S. Bell, *Physics* **1**, 195 (1964).
- [52] “Proposed Experiment to Test Local Hidden-Variable Theories”, J. F. Clauser, M. A. Horne, A. Shimony, and R. A. Holt, *Phys. Rev. Lett.* **23**, 880 (1969).
- [53] “Persistent Quantum Beats and Long-Distance Entanglement from Waveguide-Mediated Interactions”, H. Zheng and H. U. Baranger, *PRL* **110**, 113601 (2013)
- [54] “Quantum Beats from Entangled Localized Surface Plasmons”, N. Thakkar, C. Cherqui, and D. J. Masiello, *ACS Photonics*, **2** (1), pp 157-164 (2015)
- [55] “A Test of a New Type of Stellar Interferometer on Sirius”, R. Hanbury Brown and R. Q. Twiss *Nature* **178**, 1046 - 1048 (1956)